

Effect of oblique irradiation on the onset of thermal phototactic bioconvection in non-scattering medium

S. K. Rajput^{1, a)} and M. K. Panda¹

¹ *Department of Mathematics, PDPM Indian Institute of Information Technology Design and Manufacturing, Jabalpur 482005, India.*

The linear stability of a suspension of phototactic algae is investigated numerically with particular emphasis on the effects of the angle of incidence of the illuminating oblique collimated irradiation with thermal effects. The suspension is illuminated by the oblique collimated irradiation from the top and heated/cooled from the bottom. The linear stability analysis shows that the suspension becomes more unstable as the angle of incidence increases.

^{a)}Corresponding author: E-mail: shubh.iiitj@gmail.com.

I. INTRODUCTION

The phenomena of spontaneous pattern formation in suspensions of randomly, but on average upwardly swimming microorganisms are known as bioconvection¹⁻⁵. The swimming microorganisms participating in bioconvection are up to 10% denser than the medium (water here), and they are mostly algae and bacteria. Usually, bioconvection patterns are observed in the laboratory in shallow suspensions. However, these have also been found in situ in micro patches of zoo plankton. Also, bioconvection patterns disappear when the microorganisms stop swimming. Nevertheless, examples of pattern formation are also found where up-swimming and higher density are not involved. Microorganisms can adjust their swimming in response to several different environmental stimuli, which can cause them to aggregate in specific regions. These responses are known as taxes. Paradigmatic examples of taxes include gravitaxis, chemotaxis, gyrotaxis, and phototaxis. Gravitaxis refers to the response of microorganisms to gravity or acceleration, and negative gravitaxis is the swimming opposite of gravity. Responses to chemical gradients can lead to chemotaxis. Gyrotaxis is termed as the directed swimming of a bottom-heavy microorganism due to the balance between a torque due to gravity and viscous torque arising from local shear flows. Positive (negative) phototaxis is termed as the directed movement toward (away from) the dim (bright) light source, while start/stop swimming behaviour is observed in the photophobic response. The process by which the algae absorb the light incident on them directly from above and produce shadows below them is called self-shading (or shading). This manuscript is restricted to phototaxis and self-shading only.

Experimental observations have revealed that the bioconvection patterns are modified by illuminating sources of different types, for example, oblique and/or vertical collimated irradiation. The steady patterns in suspensions of (phototactic) algae may be destroyed due to strong light or their formation may be prevented in well-stirred cultures. The shape, size, symmetry, and/or scale of the bioconvection patterns can also be modified by illumination. The reason for these changes here is twofold: First, the photosynthetic pigments (e.g., chlorophyll and carotenoid) of the motile algae aid in obtaining energy during their photosynthesis. Since the motile algae are strongly phototactic, they move toward (or away from) the weak (or strong) light source via a light-seeking (or light-avoiding) behavior when $G < G_c$ (or $G > G_c$). Thereby, the cells tend to accumulate at optimal places ($G = G_c$) in their local environment. The absorption of light by the algae may be the second reason for the changes in bioconvection patterns.

The study of bioconvection has garnered significant attention across various fields, particularly focusing on the interaction between thermal and phototactic factors in microorganism suspensions. Kuznetsov⁶ delved into bio-thermal convection within suspensions of oxytactic microorganisms, while Alloui et al.⁷ investigated suspensions of mobile gravitactic microorganisms. Nield and Kuznetsov⁸ utilized linear stability analysis to explore the onset of bio-thermal convection in suspensions of gyrotactic microorganisms, and Alloui et al.⁹ scrutinized the impact of bottom heating on the onset of gravitactic bioconvection in a square enclosure. Taheri and Bilgen¹⁰ investigated the effects of bottom heating or cooling in a vertically oriented cylinder with stress-free sidewalls. Kuznetsov¹¹ developed a theoretical framework for bio-thermal convection in suspensions containing two species of microorganisms. Saini et al.¹² explored bio-thermal convection in suspensions of gravitactic microorganisms, while Zhao et al.¹³ utilized linear stability analysis to examine the stability of bioconvection in suspensions of randomly swimming gyrotactic microorganisms heated from below.

In the domain of phototactic bioconvection, Vincent and Hill¹⁴ laid the groundwork with seminal research, examining the impact of collimated irradiation on an absorbing (non-scattering) medium. Building upon this foundation, Ghorai and Hill¹⁵ extended the inquiry into the behavior of phototactic algal suspensions in two dimensions, without considering scattering effects. Subsequently, Ghorai et al.¹⁶ and Ghorai and Panda¹⁷ delved into the effects of light scattering, both isotropic and anisotropic, under normal collimated irradiation. Panda and Ghorai¹⁸ proposed a model for an isotropically scattering medium in two dimensions, yielding results divergent from those of Ghorai and Hill¹⁵ due to the inclusion of scattering effects. Panda and Singh¹⁹ explored phototactic bioconvection in two dimensions, confining a non-scattering suspension between rigid sidewalls. Additionally, Panda et al.²⁰ examined the impact of diffuse irradiation, combined with collimated irradiation, in an isotropic scattering medium, while Panda²¹ investigated an anisotropic medium. Recognizing natural environmental conditions where sunlight strikes the Earth's surface at oblique angles, Panda et al.²² studied the effects of oblique collimated irradiation on the onset of phototactic bioconvection. In a recent investigation, Panda and Rajput²³ explored the impacts of diffuse irradiation along with oblique collimated irradiation on a uniformly scattering suspension. Furthermore, Rajput and Panda²⁴ investigated the effect of scattered/diffuse flux on the onset of phototactic bioconvection in the absence of collimated flux. However, no study on the onset of thermal phototactic bioconvection that incorporates the effects of oblique collimated irradiation on an algal suspension has been hitherto carried out. Therefore, the effects of oblique collimated

irradiation on thermal bioconvection are investigated in the same vicinity.

The organization of the manuscript is as follows: The mathematical formulation of the proposed phototaxis model is described first. The basic steady state is derived next, and then, it is perturbed by infinitesimal disturbances. The linear stability problem to the basic steady state is derived next and solved numerically by taking two different cases (i.e., stress-free and rigid upper surface). Finally, the results of the numerical study are summarized and their novelty is addressed.

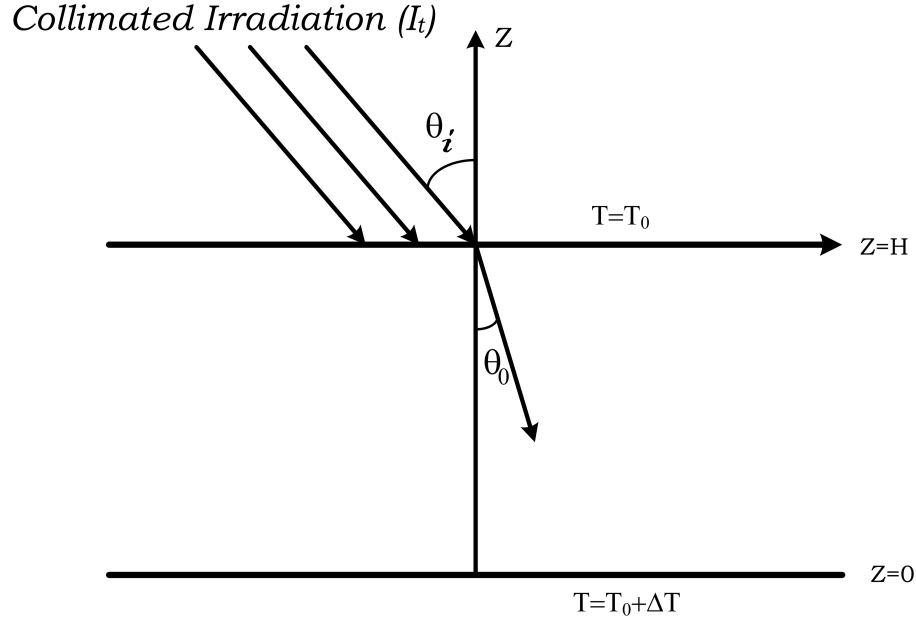


FIG. 1. Oblique collimated irradiation on the upper surface of an absorbing and non-scattering algal suspension with thermal effect on the lower surface.

II. MATHEMATICAL FORMULATION

Consider the motion in a dilute suspension of phototactic algae within a layer of finite depth H . Here, an oblique collimated irradiation illuminates the suspension from above and strikes it at a fixed off-normal angle θ_i . We choose a rectangular Cartesian coordinate system where the yz -plane is the plane of incidence for the oblique collimated irradiation. The angle of refraction θ_0 in which the collimated beam propagates across the water is determined by using Snell's law, that is, $\sin \theta_i = n_0 \sin \theta_0$. Here, n_0 denotes the refractive index of water and the estimated value for it is 1.333 approximately. Since the index of refraction of algae is not the same as that of water, the light incident on the algae across the suspension is absorbed by them and scattered

thereafter. For simplicity, the effects of scattering by algae have been neglected in the present study. Let $I(\mathbf{x}, \mathbf{s})$ represent the radiation intensity propagating in the (unit) direction $\mathbf{s} = \cos \theta \hat{z} + \sin \theta (\cos \phi \hat{x} + \sin \phi \hat{y})$ at a position \mathbf{x} across the algal suspension, where \mathbf{x} is measured relative to a rectangular cartesian coordinate system with the z axis vertically up. Here, θ denotes the polar angle (measured from the z axis) and ϕ denotes the azimuthal angle (measured in between the projection of the radiation intensity onto xy - plane and the x axis) describing the unit vector

$$\mathbf{x}$$

(in spherical polar coordinate system).

III. PHOTOTAXIS COUPLED WITH SELF-SHADING IN SUSPENSIONS OF ALGAE

We assume here that the medium across the algal suspension is absorbing and non-scattering similar to Vincent and Hill. To calculate light intensity profiles, the radiative transfer equation (hereafter referred to as RTE) is given by

$$\mathbf{s} \cdot \nabla I(\mathbf{x}, \mathbf{s}) + \kappa I(\mathbf{x}, \mathbf{s}) = 0 \quad (1)$$

where κ is the absorption coefficient.

The collimated intensity at location $\mathbf{x}_b = (x, y, H)$ (i.e., the top boundary surface) is expressed by using a Dirac delta function as

$$I(\mathbf{x}_b, \mathbf{s}) = I_t \delta(\mathbf{s} - \mathbf{s}_0).$$

Here, I_t is the magnitude of oblique collimated irradiation and $\mathbf{s}_0 = \sin(\pi - \theta_0) \cos \phi \hat{x} + \sin(\pi - \theta_0) \sin \phi \hat{y} + \cos(\pi - \theta_0) \hat{z}$ is the incident direction defined in spherical polar coordinates. Also, \hat{x} , \hat{y} , and \hat{z} are unit vectors along the x , y , and z axes. The Dirac-delta function δ satisfies

$$\int_0^{4\pi} f(\mathbf{s}) \delta(\mathbf{s} - \mathbf{s}_0) = f(\mathbf{s}_0).$$

The absorption coefficient is linearly proportional to the concentration n so that $\kappa = \varkappa n$, and thus, the RTE in a non-scattering and absorbing suspension becomes

$$\mathbf{s} \cdot \nabla I(\mathbf{x}, \mathbf{s}) + \varkappa n I(\mathbf{x}, \mathbf{s}) = 0 \quad (2)$$

The total intensity, $G(\mathbf{x})$; at a point \mathbf{x} in the medium is

$$G(\mathbf{x}) = \int_0^{4\pi} I(\mathbf{x}, \mathbf{s}) d\Omega. \quad (3)$$

The radiative heat flux, $\mathbf{q}(\mathbf{x})$, at a point \mathbf{x} in the medium is

$$\mathbf{q}(\mathbf{x}) = \int_0^{4\pi} I(\mathbf{x}, \mathbf{s}) \mathbf{s} d\Omega. \quad (4)$$

Let \mathbf{p} be the unit vector pointing in the swimming direction of a cell. The mean swimming direction, $\langle \mathbf{p} \rangle$, is defined as the ensemble average of the swimming direction and \mathbf{p} for all the cells in a small volume. The swimming speed does not depend on the illumination, position, time, and direction of many species of microorganisms. It is assumed that the cells swim at the same speed relative to the fluid. We denote the ensemble average swimming speed by W_c . The average swimming velocity is, thus,

$$\langle \mathbf{p} \rangle = M(G) \hat{\mathbf{z}}. \quad (5)$$

Here, $M(G)$ is the phototaxis function, which represents the response of algae to light, and mathematically, it is defined as

$$M(G) = \begin{cases} \geq 0, & \text{when } G \leq G_c, \\ < 0, & \text{when } G > G_c. \end{cases}$$

IV. GOVERNING EQUATIONS

In common with the previous models of bioconvection, we assume a monodisperse cell population that can be modelled by a continuous distribution. The suspension is diluted so that the volume fraction of the cells is small and cell–cell interactions are negligible. Each cell has a volume ϑ and density $\rho + \Delta\rho$, ρ is the density of the fluid in which the cells swim and $\Delta\rho \ll \rho$. Let \mathbf{u} and n , respectively, denote the fluid velocity and concentration in the suspension. Supposing that the suspension is incompressible, conservation of mass implies

$$\nabla \cdot \mathbf{u} = 0. \quad (6)$$

We assume that the Stokeslet due to the negative buoyancy of the cells is dominant and all other contributions of the cells to the bulk stress are negligible. Thus, neglecting all effects on the fluid

except the cells' negative buoyancy, the momentum equation under the Boussinesq approximation is

$$\rho \left(\frac{D\mathbf{u}}{Dt} \right) = -\nabla P_e + \mu \nabla^2 \mathbf{u} - n \vartheta g \Delta \rho \hat{\mathbf{z}} - \rho g (1 - \beta(T - T_0)) \hat{\mathbf{z}}. \quad (7)$$

where P_e is the excess pressure above the hydrostatic pressure, g is the acceleration due to gravity, and μ is the viscosity of the suspension, which is assumed to be that of the fluid. Here, D/Dt is the material time derivative and β is the coefficient of thermal expansion.

The equation for cell conservation is

$$\frac{\partial n}{\partial t} = -\nabla \cdot \mathbf{F}, \quad (8)$$

where the flux of cells is

$$\mathbf{F} = n(\mathbf{u} + W_c \langle \mathbf{p} \rangle) - \mathbf{D} \cdot \nabla n.$$

The first term on the right-hand side of Eq. (7) is the flux due to the advection of the cells by the bulk fluid flow. The second term arises due to the average swimming velocity of the cells. The third term represents the random component of the cell locomotion. We choose the diffusivity tensor \mathbf{D} to be isotropic and constant. Thus, $\mathbf{D} = DI$, where D is the diffusion coefficient and I is the identity tensor. Thus, the flux of cells becomes

$$\mathbf{F} = n(\mathbf{u} + W_c \langle \mathbf{p} \rangle) - D \cdot \nabla n.$$

Here, each algal cell is idealized as a homogeneous spherical body having a uniform distribution of mass and purely phototactic, and thus, its centre of gravity and centre of buoyancy coincide (i.e., the torque due to gravity does not exist). Two major assumptions have been made in deriving the cell flux vector in the proposed model. First, since the algal cells are purely phototactic, the effect of viscous torque due to shear in the flow, which might contribute to the horizontal component of the mean swimming orientation, is neglected. It can be justified clearly from the linear stability theory that the perturbed vorticity, and hence the viscous torque, is infinitesimally small. Hence, the viscous reorientation can be neglected on the limit. Second, the diffusion tensor, which should be a function of light intensity, is assumed to be a constant isotropic tensor, instead of deriving it from a swimming velocity autocorrelation function. Thus, this model can be considered to be valid in the limiting case, to understand the complexities of bioconvection

due to phototaxis before exploring more detailed complex models. These assumptions allow us to eliminate the Fokker–Planck equation (which relates the degree of alignment of phototactic algae with the fluid below) from the governing system for phototactic bioconvection.

Also, the thermal energy equation

$$\rho c \left[\frac{\partial T}{\partial t} + \nabla \cdot (\mathbf{u}T) \right] = \alpha \nabla^2 T, \quad (9)$$

where ρc is the volumetric heat capacity of water, and α is the thermal conductivity of water.

V. BOUNDARY CONDITIONS

The lower boundary ($z = 0$) is taken as rigid, while the upper boundary ($z = H$) may be stress-free or rigid. Since there is no flux of cells at each boundary, the boundary conditions are

$$\mathbf{u} = \mathbf{F} \cdot \hat{\mathbf{z}} = 0 \quad \text{on } z = 0, \quad (10a)$$

$$\mathbf{u} \cdot \hat{\mathbf{z}} = \mathbf{F} \cdot \hat{\mathbf{z}} = 0 \quad \text{on } z = H, \quad (10b)$$

for rigid boundaries

$$\mathbf{u} \times \hat{\mathbf{z}}^* = 0 \quad \text{on } z = 0, H, \quad (10c)$$

while for a free boundary

$$\frac{\partial^2}{\partial z^2} (\mathbf{u} \times \hat{\mathbf{z}}) = 0 \quad \text{on } z = H, \quad (10d)$$

for temperature on both boundaries

$$T = T_0 + \Delta T \quad \text{on } z = 0, \quad (10e)$$

$$T = T_0 \quad \text{on } z = H. \quad (10f)$$

The top boundary is exposed to a uniform oblique solar irradiation of magnitude I_t . The top and the bottom boundaries are also assumed to be non-reflecting, thus,

$$\text{at } z = H, \quad I(x, y, z, \theta, \phi) = I_t \delta(\mathbf{s}, \mathbf{s}_0) \quad (\pi/2 \leq \theta \leq \pi).$$

$$\text{at } z = 0, \quad I(x, y, z, \theta, \phi) = 0 \quad (0 \leq \theta \leq \pi/2).$$

VI. SCALING OF THE EQUATIONS

The governing system for bioconvection can be made dimensionless by scaling all lengths on H , the depth of the layer, time on diffusive timescale H^2/α_f , and the bulk fluid velocity on α_f/H . The appropriate scaling for the pressure is $\mu\alpha_f/H^2$; the cell concentration is scaled \bar{n} , the mean concentration; and temperature is scaled by $(T - T_0)/\Delta T$. For convenience, we keep the same on n notation for the dimensional and nondimensional variables. The recasting of the governing system for bioconvection in terms of the nondimensional variables is as follows

$$\nabla \cdot \mathbf{u} = 0, \quad (11)$$

$$P_r^{-1} \left(\frac{D\mathbf{u}}{Dt} \right) = -\nabla P_e + \nabla^2 \mathbf{u} - R_b n \hat{\mathbf{z}} - R_m \hat{\mathbf{z}} + R_T T \hat{\mathbf{z}}, \quad (12)$$

$$\frac{\partial n}{\partial t} = -\nabla \cdot \mathbf{F}, \quad (13)$$

where the flux of cells is

$$\mathbf{F} = n\mathbf{u} + \frac{1}{Le} n \mathbf{V}_c \langle p \rangle - \frac{1}{Le} \nabla n, \quad (14)$$

$$\frac{\partial T}{\partial t} + \nabla \cdot (\mathbf{u}T) = \nabla^2 T. \quad (15)$$

Here, $P_r = \nu/\alpha_f$ is the Prandtl number, $V_c = W_s H/D$ is the scaled swimming speed, $R_b = \bar{n} \nu g \Delta \rho H^3 / \mu \alpha_f$ is the bioconvective Rayleigh number, $R_T = g \beta \Delta T H^3 / \mu \alpha_f$ is the thermal Rayleigh number and $R_m = \rho g H^3 / \mu \alpha_f$ is the basic density Rayleigh number and Lewis number $Le = \alpha_f / D$. Here, α_f is the thermal diffusivity of water. In dimensionless form, the boundary conditions become

$$\mathbf{u} = \mathbf{F} \cdot \hat{\mathbf{z}} = 0 \quad \text{on } z = 0, \quad (16a)$$

$$\mathbf{u} \cdot \hat{\mathbf{z}} = \mathbf{F} \cdot \hat{\mathbf{z}} = 0 \quad \text{on } z = 1, \quad (16b)$$

for rigid boundaries

$$\mathbf{u} \times \hat{\mathbf{z}} = 0 \quad \text{on } z = 0, 1, \quad (16c)$$

while for a free boundary

$$\frac{\partial^2}{\partial z^2} (\mathbf{u} \times \hat{\mathbf{z}}) = 0 \quad \text{on } z = 1, \quad (16d)$$

for temperature on both boundaries

$$T = T_0 + \Delta T \quad \text{on } z = 0, \quad (16e)$$

$$T = T_0 \quad \text{on} \quad z = 1. \quad (16f)$$

In terms of the nondimensional variables, the RTE [see Eq. (2)] becomes

$$\mathbf{s} \cdot \nabla I(\mathbf{x}, \mathbf{s}) + \kappa_H I(\mathbf{x}, \mathbf{s}) = 0 \quad (17)$$

where $\kappa_H = \kappa \bar{n} H$ is the (vertical) optical depth of the suspension. In dimensionless form, the intensity at the top and bottom becomes

$$I(x, y, z = 1, \theta, \phi) = I_t \delta(\mathbf{s} - \mathbf{s}_0), \quad (\pi/2 \leq \theta \leq \pi), \quad (18)$$

$$I(x, y, z = 0, \theta, \phi) = 0, \quad (0 \leq \theta \leq \pi/2), \quad (19)$$

VII. THE BASIC SOLUTION

Equations (11)–(15) and Eq. (17) together with the boundary conditions possess a static equilibrium solution in which

$$\mathbf{u} = 0, \quad n = n_s(z), \quad T = T_s(z) \quad \text{and} \quad I = I_s(z, \theta).$$

The total intensity G_s at the basic state is given by

$$G_s = \int_0^{4\pi} I_s(z, \theta) d\Omega.$$

If horizontal homogeneity and azimuthally isotropic are assumed (as considered here), the RTE becomes

$$\frac{dI_s(z, \theta)}{dz} + \frac{\tau_H n_s I_s(z, \theta)}{\cos \theta} = 0, \quad (20)$$

subject to the top boundary condition

$$I_s(1, \theta) = I_t \delta(\mathbf{s} - \mathbf{s}_0). \quad (21)$$

Solving Eqs. (20) and (21), we get

$$dI_s(z, \theta) = I_t \delta(\mathbf{s} - \mathbf{s}_0) \exp\left(\int_z^1 \frac{\tau_H n_s(z')}{\cos \theta} dz'\right), \quad (22)$$

The basic total intensity is written as

$$G_s(z) = \int_0^{4\pi} I_s(z, \theta) d\Omega = I_t \exp\left(\frac{-\int_z^1 \tau_H n_s(z') dz'}{\cos \theta_0}\right). \quad (23)$$

Now, the radiative heat flux, $\mathbf{q}_s(z)$, in basic state is given by

$$\mathbf{q}_s(z) = \int_0^{4\pi} I_s(z, \theta) \hat{\mathbf{s}} d\Omega.$$

The radiative heat flux normal to the boundary surfaces of the algal suspension is given by

$$(\mathbf{q}_s \cdot \hat{\mathbf{z}}) \hat{\mathbf{z}} = \left[I_t \exp\left(\frac{-\tau_H \int_z^1 n_s(z') dz'}{\cos \theta_0}\right) \cos \theta_0 \right] (-\hat{\mathbf{z}})$$

Since the illuminating source lies in the opposite direction to the radiative heat flux vector, the mean swimming direction in the basic state is expressed as

$$\langle \mathbf{p}_s \rangle = M_s \hat{\mathbf{z}} \quad \text{where } M_s = M(G).$$

The basic concentration, $n_s(z)$, satisfies

$$\frac{dn_s}{dz} - V_c M_s n_s = 0, \quad (24)$$

which is supplemented by the cell conservation relation

$$\int_0^1 n_s(z) dz = 1. \quad (25)$$

The basic temperature $T_s(z)$ is satisfied satisfy

$$\frac{d^2 T_s}{dz^2} = 0. \quad (26)$$

where

$$T_s - 1 = 0, \quad \text{at } z = 0 \quad (27)$$

$$T_s = 0, \quad \text{at } z = 1. \quad (28)$$

By introducing a new variable $\varpi = \int_1^z n_s dz$, Eq. (25) becomes

$$\frac{d^2 \varpi}{dz^2} - V_c T_s \frac{d\varpi}{dz} = 0, \quad (29)$$

with boundary condition

$$\bar{\omega} + 1 = 0, \text{ at } z = 0 \quad (30)$$

$$\bar{\omega} = 0, \text{ at } z = 1. \quad (31)$$

In terms of $\bar{\omega}$, the basic total intensity G_s can be expressed as

$$G_s(z) = I_t \exp\left(\frac{\tau_H \bar{\omega}}{\cos \theta_0}\right)$$

Equations (26) and (29) with specific boundary conditions constitute a boundary value problem, which is solved numerically using a shooting method.

VIII. LINEAR STABILITY OF THE PROBLEM

To perform linear stability analysis, the basic state is perturbed via infinitesimal disturbances as

$$\begin{pmatrix} \mathbf{u} \\ n \\ T \\ \langle \mathbf{I} \rangle \end{pmatrix} = \begin{pmatrix} 0 \\ n_s \\ T_s \\ \langle \mathbf{I}_s \rangle \end{pmatrix} + \varepsilon \begin{pmatrix} \mathbf{u}_1 \\ n_1 \\ T_1 \\ \langle \mathbf{I}_1 \rangle \end{pmatrix} + O(\varepsilon^2), \quad (32)$$

where $\mathbf{u}_1 = (u_1, v_1, w_1)$.

The linearized equations about the basic state are

$$\nabla \cdot \mathbf{u}_1 = 0, \quad (33)$$

$$P_r^{-1} \left(\frac{\partial \mathbf{u}_1}{\partial t} \right) = -\nabla P_e + \nabla^2 \mathbf{u}_1 - R_b n_1 \hat{z} + R_T T_1 \hat{z}, \quad (34)$$

$$\frac{\partial n_1}{\partial t} + \frac{1}{Le} V_c \nabla \cdot (\langle \mathbf{p}_s \rangle n_1 + \langle \mathbf{p}_1 \rangle n_s) + w_1 \frac{dn_s}{dz} = \frac{1}{Le} \nabla^2 n_1, \quad (35)$$

$$\frac{\partial T_1}{\partial t} - w_1 \frac{dT_s}{dz} = \nabla^2 T_1. \quad (36)$$

Now the total intensity, G , is given by

$$G_s(z) = I_t \left[\frac{\int_1^z (\tau_H n_s(z) + \varepsilon n_1 + O(\varepsilon^2)) dz'}{\cos \theta_0} \right]$$

The steady intensity is perturbed, and after simplification, we get

$$G = G_s + \varepsilon G_1 + O(\varepsilon^2)$$

where

$$G_1 = I_t \exp\left(\frac{\int_1^z \tau_H n_s(z') dz'}{\cos \theta_0}\right) \left(\frac{\int_1^z \tau_H n_1 dz'}{\cos \theta_0}\right), \quad (37)$$

Hence, the perturbed mean swimming orientation [i.e., $T(G)\hat{z}$] at $O(\varepsilon^2)$ for a non-scattering algal suspension is expressed as

$$\langle \mathbf{p}_1 \rangle = G_1 \frac{dM_s}{dG} \hat{z}. \quad (38)$$

We eliminate P_e and the horizontal component of \mathbf{u}_1 by taking the curl of Eq. (34) twice and retaining the z -component of the result. Then, Eqs. (33)–(37) reduce to two equations for w_1 and n_1 . Now, this equation can be decomposed into normal mode as

$$\begin{pmatrix} w_1 \\ n_1 \\ T_1 \end{pmatrix} = \begin{pmatrix} W(z) \\ \Theta(z) \\ T(z) \end{pmatrix} + \exp[\sigma t + i(k_x x + k_y y)], \quad (39)$$

$W(z)$, $\Theta(z)$, and $T(z)$ represent the variations in the z direction, while k_x and k_y are the horizontal wavenumbers. The complex growth rate of the disturbances is denoted by σ .

The linear stability equations become

$$\left(\sigma P_r^{-1} + k^2 - \frac{d^2}{dz^2}\right) \left(\frac{d^2}{dz^2} - k^2\right) W = R_b k^2 \Theta - R_T k^2 T, \quad (40)$$

$$\left(\sigma Le + k^2 - \frac{d^2}{dz^2}\right) \Theta + \mathfrak{N}_0(z) \int_z^1 \Theta dz + \mathfrak{N}_1(z) \Theta + \mathfrak{N}_2(z) \frac{d\Theta}{dz} = -Le \frac{dn_s}{dz} W, \quad (41)$$

$$\left(\frac{d^2}{dz^2} - k^2 - \gamma\right) T(z) = \frac{dT_s}{dz} W(z), \quad (42)$$

where

$$\mathfrak{N}_0(z) = -(\tau_H / \cos \theta_0) V_c \frac{d}{dz} \left(n_s G_s^c \frac{dM_s}{dG} \right), \quad (43a)$$

$$\mathfrak{N}_1(z) = 2(\tau_H / \cos \theta_0) V_c n_s G_s \frac{dM_s}{dG}, \quad (43b)$$

$$\mathfrak{N}_2(z) = V_c M_s. \quad (43c)$$

subject to the boundary conditions

$$W = \frac{dW}{dz} = \frac{d\Theta}{dz} - \mathfrak{K}_2(z)\Theta - n_s V_c (\tau_H / \cos \theta_0) G_s \left(\int_z^1 \Theta dz \right) \frac{dM_s}{dG} = 0, \text{ at } z = 0, \quad (44)$$

$$W = \frac{d^2W}{dz^2} = \frac{d\Theta}{dz} - \mathfrak{K}_2(z)\Theta = 0, \text{ at } z = 1. \quad (45)$$

At a rigid upper surface, the condition in Eq. (45) is replaced by

$$W = \frac{dW}{dz} = \frac{d\Theta}{dz} - \mathfrak{K}_2(z)\Theta = 0, \text{ at } z = 1. \quad (46)$$

Here, $k = \sqrt{k_x^2 + k_y^2}$ is the horizontal wavenumber and it represents the modulation of the bioconvection pattern in horizontal directions. Equations (40)-(42) form an eigenvalue problem for σ as a function of the dimensionless parameters θ_0 , k , P_r , V_c , τ_H , R_b and R_T . The basic state becomes unstable whenever $Re(\sigma) > 0$.

Introducing a new variable

$$\Phi(z) = \int_z^1 \Theta(z') dz', \quad (47)$$

the linear stability equations become (writing $D = d/dz$)

$$D^4W - (2k^2 + \sigma Le P_r^{-1})D^2W + k^2(k^2 + \sigma Le P_r^{-1})W = -R_b k^2 D\Phi + R_T k^2 T(z), \quad (48)$$

$$D^3\Phi - \mathfrak{K}_3(z)D^2\Phi - (\sigma Le + k^2 + \mathfrak{K}_2(z))D\Phi - \mathfrak{K}_1(z)\Phi - \mathfrak{K}_0(z) = Le Dn_s W, \quad (49)$$

$$(D^2 - k^2 - \sigma)T(z) = DT_s W, \quad (50)$$

with

$$W = DW = D^2\Phi - \mathfrak{K}_2(z)D\Phi - n_s V_c (\tau_H / \cos \theta_0) G_s \frac{dM_s}{dG} \Phi = 0, \text{ at } z = 0, \quad (51)$$

$$W = D^2W = D^2\Phi - \mathfrak{K}_2(z)D\Phi = 0, \text{ at } z = 1. \quad (52)$$

At a rigid upper surface, the condition in Eq. (37) is replaced by

$$W = DW = D^2\Phi - \mathfrak{K}_2(z)D\Phi = 0, \text{ at } z = 1. \quad (53)$$

$$T(z) = 0, \text{ at } z = 0, 1. \quad (54)$$

There is also an extra boundary condition

$$\Phi(z) = 0, \quad \text{at } z = 1. \quad (55)$$

which follows from Eq. (47). The new aspects of the proposed model via the effects of oblique collimated irradiation are incorporated in the terms \aleph_2 , \aleph_2 , and \aleph_2 , which are found on the perturbed cell conservation equation, Eq. (49).

IX. SOLUTION PROCEDURE

Numerical solutions to Eqs. (48) - (50) with appropriate boundary conditions are calculated with a fourth-order accurate, finite-difference scheme based on Newton–Raphson–Kantorovich (NRK) iterations. This NRK routine solves a system of first-order, nonlinear, coupled, ordinary differential equations (ODEs) resulting from the two-point boundary value problem. In the NRK routine, a guess is required for the solution of the system of ordinary differential equations (ODEs). Next, the guess is refined by successive iterations until the desired accuracy is reached. The numerical results are checked for accuracy by comparing the solution computed by the NRK routine (used in this study) of a benchmark problem in the same vicinity with another (solution) calculated by a routine, which is different from the former (NRK routine), such as the solution of the mixed-convection flow in a vertical pipe. It reveals that the solution generated by the said routine (NRK) is in excellent agreement with the one, which utilizes the Chebyshev collocation method (see Table I of Ref. 39 for details). Furthermore, the numerical scheme is tested for many different parameters and mesh sizes. It shows that the solutions obtained using the scheme for the same parameters on different meshes always agree to 5 (or more) significant figures for a minimum of 51 mesh points. This numerical scheme (NRK routine) is utilized to calculate the neutral stability curves (or neutral curves) in the (k, R) -plane, where $R = (R_b, R_T)$ or the growth rate, $Re(\sigma)$, as a function of R for a fixed set of other parameters. Initially, the values of P_r , V_c , τ_H , θ_0 , and k are supplied, and the values of W , Φ and T are estimated either from the previous numerical results or by imposing sinusoidal variation in W , Φ and T . Once a solution is obtained, this solution can be used as an initial guess for the neighbouring parameter values.

For a given set of other parameters, there are an infinite number of branches of the neutral curve $R^{(n)}(k)$, with $n = 1, 2, 3, \dots$; each one representing a particular solution of the linear stability problem. The solution branch of most interest is the one on which R has its minimum value R^c and the corresponding bioconvective solution, that is, (k^c, R^c) , where R^c is either R_b^c or R_T^c is called

the most unstable solution. The wavelength of the initial disturbance can be calculated from it by using the relation $\lambda_c = 2\pi/k^c$. Please note here that the linear stability theory is expected to explain the initial bioconvection pattern spacing before the nonlinear effects in the system become dominant. Solutions consist of convection cells stacked one above another along the depth of the suspension. A solution is said to be of mode n if it has n convection cells stacked vertically one on another. In many instances, the most unstable solution occurs on the $R^{(n)}(k)$ branch of the neutral curve and it is mode 1.

A neutral curve is defined as the locus of points where $Re(\sigma) = 0$. If in addition $Im(\sigma) = 0$ on such a curve, then the principle of exchange of stabilities is said to be valid and the bioconvective solution is called stationary (non-oscillatory). Alternatively, if $Im(\sigma) \neq 0$ then oscillatory solutions exist. If the most unstable solution remains on the oscillatory branch of the neutral curve, then the solution is called overstable. When there is competition between the stabilizing and destabilizing processes, the oscillatory solution evolves. In this instance, a single oscillatory branch bifurcates from the stationary branch of the corresponding neutral curve at some $k = k_b$ and exists for $k < k_b$.

To estimate the parameters required for the present study, we assume that we are dealing with a phototactic microorganism similar to *Chlamydomonas*. To retain the resulting model to be more rational and can be comparable with earlier studies on (phototactic) bioconvection, we use the same parameter values as taken by Refs. 17, 22, and 40. Accounting for refraction at the air-water interface, the range of the declination angle θ_0 is restricted such that $0.661 \leq \cos \theta_0 \leq 1.0$; and this implies that $0 \leq \theta_i(deg) \leq 48.6$ approximately. Following Daniel et al., we have estimated the approximate range of the angle of incidence θ_i as $0 \leq \theta_i \leq 80$ for our proposed model. The radiation characteristics required here are calculated as given in Ghorai and Panda. Thus, for a 0.50cm deep suspension, optical depth τ_H varies in the range from 0.25 to 1. The scaled swimming speed can be calculated for a 0.5 and 1.0cm deep suspension as $V_c = 10$ and $V_c = 20$, respectively.

X. NUMERICAL RESULTS

We have systematically investigated the effects of the angle of incidence θ_i on the base concentration profiles and the corresponding neutral curves by varying it via discrete values, keeping the other governing parameters fixed. The values of $Pr = 5$ and $I_t = 0.8$ are kept fixed throughout to compare our model with the existing rational models on (phototactic) bioconvection. The representative values of the cell swimming speed and the optical (vertical) depth are $V_c = 10, 15,$

20, and $\tau_H = 0.5, 1.0$, respectively. The value of the critical total intensity G_c is selected such that the maximum basic concentration occurs at around mid-height of the suspension domain, while the angle of incidence remains fixed as $\theta_i = 0$ (i.e., vertical collimated irradiation case). Then, the angle of incidence $\theta_i \in [0 : 80]$ is varied discretely with an increment of 10 starting from 0 and we study their effects on the bioconvection patterns at instability. Please note that due to a large number of parameter values, it is very difficult to obtain a comprehensive picture across the whole parameter domain. Thus, we have taken a discrete set of fixed parameter values to study their effects on the onset of bioconvection. We determine the bioconvective Rayleigh number, R_b , at the onset of bioconvection as a function of wavenumber, k , for various thermal Rayleigh numbers, R_T . We also divide the obtained results into two categories based on the suspension top boundary condition (e.g., stress-free or rigid). Then, we address them separately by taking two cases.

XI. CASE I: STRESS-FREE UPPER SURFACE

To study the effects of angle of incidence on the onset of bioconvection, here we consider the case when the upper surface of the algal suspension is stress-free.

In Fig. 2, we show the neutral curves at the variation in the angle of incidence as $\theta_i = 0, 20, 30, 40, 60$, and 80 , respectively, while keeping the other governing parameters $V_c = 10$; $\tau_H = 0.5$, $R_T = 50$ and $G_c = 0.63$ fixed. When $\theta_i = 0$, the maximum basic concentration occurs at around mid-height of the domain resulting into a horizontal concentrated sublayer. The region below (above) the sublayer is gravitationally unstable (locally stable). As the value of θ_i is increased up to 80 , the location of the maximum basic concentration (i.e., sublayer) shifts toward the top of the domain, and simultaneously, the value of maximum basic concentration increases. The width of the upper (lower) stable (unstable) region gradually decreases (increases) at the same time. Thereby, the buoyancy of the upper stable fluid does not inhibit to convection adequately, whereas the lower unstable convective region supports it very strongly due to a substantial increase in its height. Eventually, both the critical wavenumber k^c and bioconvective Rayleigh number R_b^c at bioconvective instability decrease and thus, the suspension becomes more unstable as the angle of incidence θ_i is increased to higher non-zero values [see Fig. 2].

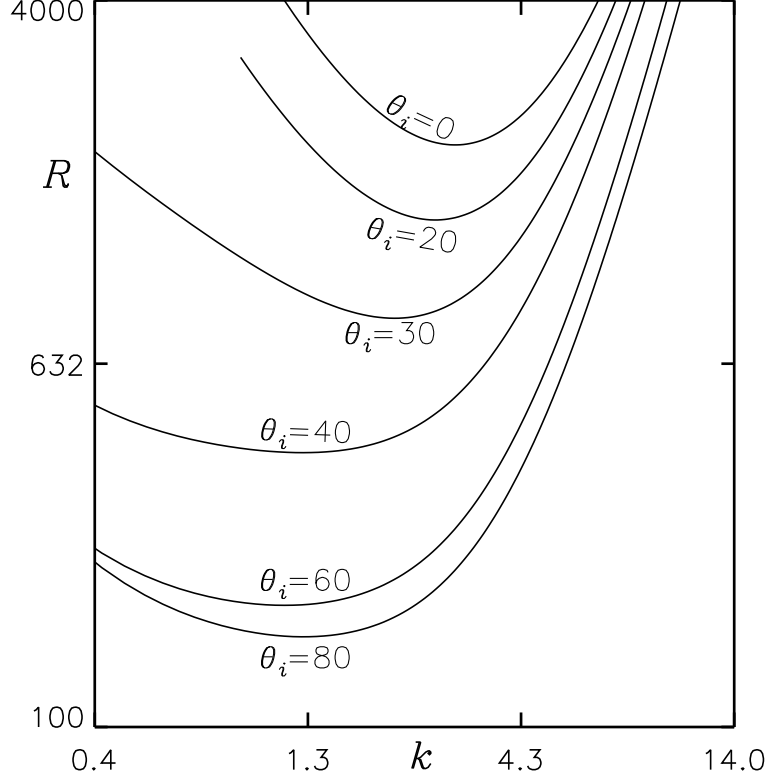


FIG. 2. The Neutral curves for various values of the angle of incidence θ_i . Here, the upper surface is stress-free and the other governing parameters $V_c = 10$, $\tau_H = 0.5$ and $R_T = 50$ are fixed.

XII. CASE-II: RIGID UPPER SURFACE

To emphasize the comparison between the theoretical predictions of the proposed model on bioconvection and the corresponding quantitative studies, we analyze here the solutions at the instability in a suspension of phototactic algae contained between two rigid surfaces located at $z = 0$ and $z = 1$, respectively. It may also be interesting to know that the collection of cells at the top surface may form a rigid-like packed layer if the upper boundary is open to the air medium.

Figure 3 shows the neutral curves at the variation in the angle of incidence as $\theta_i = 0, 20, 40, 60, \text{ and } 80$, respectively, while the other governing parameters $V_c = 10$; $\tau_H = 0.1$, $R_T = 50$ and $G_c = 0.495$ fixed. remain constant. At $\theta_i = 0$, the location of the maximum basic concentration is around the mid-height of the chamber and the corresponding stationary branch of the neutral curve possesses the most unstable solution leading the bioconvective solution to be non-oscillatory (stationary). As θ_i is increased further to higher non-zero values, the location of the maximum basic concentration shifts toward the top of the chamber and simultaneously the value of maximum

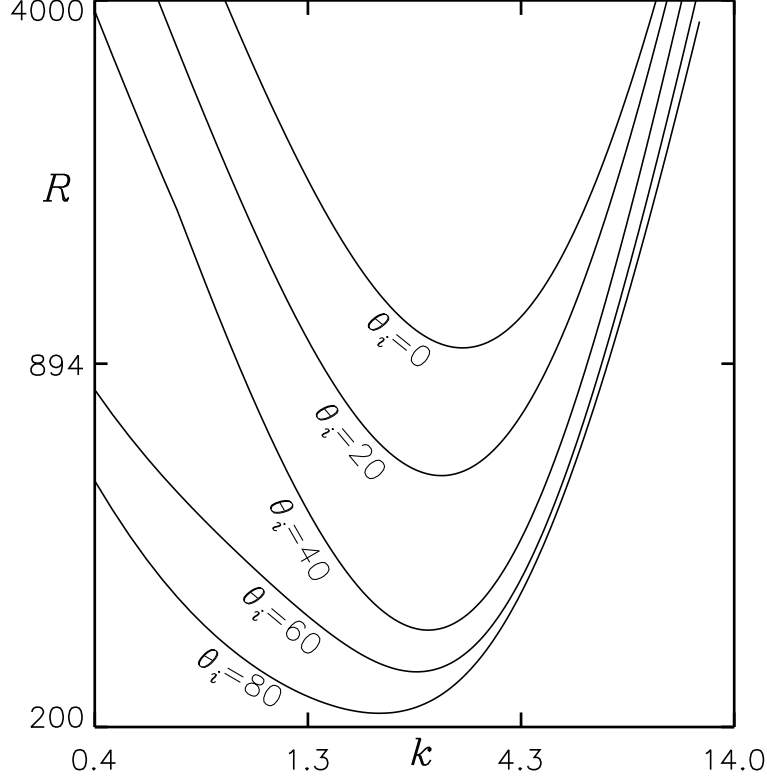


FIG. 3. The Neutral curves for various values of the angle of incidence θ_i . Here, the upper surface is rigid and the other governing parameters $V_c = 10$, $\tau_H = 1$ and $R_T = 50$ are fixed.

concentration increases. The most unstable solution tends to remain in the stationary branch of the neutral curve as θ_i is increased up to 80. The width of the upper (lower) stable (unstable) region gradually decreases (increases) at the same time. Thereby, the buoyancy of the upper stable fluid does not inhibit convection adequately, whereas the lower unstable convective region supports it very strongly due to a substantial increase in its height. Eventually, both the critical wavenumber k^c and bioconvective Rayleigh number R_b^c at bioconvective instability decrease and thus, the suspension becomes more unstable as the angle of incidence θ_i is increased to higher non-zero values [see Fig. 3].

XIII. CONCLUSION

In this innovative model of thermal bioconvection driven by thermal effect and phototaxis, we investigate the emergence of bio-thermal convection within a suspension comprising non-scattering phototactic algae. The oblique collimated irradiation strikes the suspension top at a

fixed angle of incidence. The linear stability of the suspension has been analyzed using this model. In the basic state, it is observed that self-shading becomes dominant (via increment in slant-path length) at the increment in angle of incidence, and thus, the algae receive light of low intensities (via variation in angle of incidence) at a fixed interior depth. Thereby, the location of maximum basic concentration shifts toward the suspension top and the value of maximum basic concentration increases at the increment in angle of incidence. When the value of optical depth is higher, the base concentration profiles become steeper as the angle of incidence is increased, while keeping the other governing parameters fixed.

Linear stability analysis predicts that the perturbation to the basic steady state is either stationary or oscillatory (overstable). Furthermore, the critical Rayleigh number usually decreases as the angle of incidence is increased. As a result, the algal suspension becomes more unstable at the increment in angle of incidence.

AVAILABILITY OF DATA

The supporting data of this article is available within the article.

REFERENCES

REFERENCES

- ¹J. R. Platt, “" bioconvection patterns" in cultures of free-swimming organisms,” *Science* **133**, 1766–1767 (1961).
- ²T. J. Pedley and J. O. Kessler, “Hydrodynamic phenomena in suspensions of swimming microorganisms,” *Annual Review of Fluid Mechanics* **24**, 313–358 (1992).
- ³N. A. Hill and T. J. Pedley, “Bioconvection,” *Fluid Dynamics Research* **37**, 1 (2005).
- ⁴M. A. Bees, “Advances in bioconvection,” *Annual Review of Fluid Mechanics* **52**, 449–476 (2020).
- ⁵A. Javadi, J. Arrieta, I. Tuval, and M. Polin, “Photo-bioconvection: towards light control of flows in active suspensions,” *Philosophical Transactions of the Royal Society A* **378**, 20190523 (2020).
- ⁶A. V. Kuznetsov, “Thermo-bioconvection in a suspension of oxytactic bacteria,” *International communications in heat and mass transfer* **32**, 991–999 (2005).

- ⁷Z. Alloui, T. H. Nguyen, and E. Bilgen, “Stability analysis of thermo-bioconvection in suspensions of gravitactic microorganisms in a fluid layer,” *International communications in heat and mass transfer* **33**, 1198–1206 (2006).
- ⁸D. Nield and A. Kuznetsov, “The onset of bio-thermal convection in a suspension of gyrotactic microorganisms in a fluid layer: oscillatory convection,” *International journal of thermal sciences* **45**, 990–997 (2006).
- ⁹Z. Alloui, T. Nguyen, and E. Bilgen, “Numerical investigation of thermo-bioconvection in a suspension of gravitactic microorganisms,” *International journal of heat and mass transfer* **50**, 1435–1441 (2007).
- ¹⁰M. Taheri and E. Bilgen, “Thermo-bioconvection in a suspension of gravitactic micro-organisms in vertical cylinders,” *International journal of heat and mass transfer* **51**, 3535–3547 (2008).
- ¹¹A. Kuznetsov, “Bio-thermal convection induced by two different species of microorganisms,” *International Communications in Heat and Mass Transfer* **38**, 548–553 (2011).
- ¹²S. Saini and Y. Sharma, “Analysis of onset of bio-thermal convection in a fluid containing gravitactic microorganisms by the energy method,” *Chinese journal of physics* **56**, 2031–2038 (2018).
- ¹³M. Zhao, Y. Xiao, and S. Wang, “Linear stability of thermal-bioconvection in a suspension of gyrotactic micro-organisms,” *International Journal of Heat and Mass Transfer* **126**, 95–102 (2018).
- ¹⁴R. V. Vincent and N. A. Hill, “Bioconvection in a suspension of phototactic algae,” *Journal of Fluid Mechanics* **327**, 343–371 (1996).
- ¹⁵S. Ghorai and N. A. Hill, “Penetrative phototactic bioconvection,” *Physics of fluids* **17**, 074101 (2005).
- ¹⁶S. Ghorai, M. K. Panda, and N. A. Hill, “Bioconvection in a suspension of isotropically scattering phototactic algae,” *Physics of Fluids* **22**, 071901 (2010).
- ¹⁷S. Ghorai and M. K. Panda, “Bioconvection in an anisotropic scattering suspension of phototactic algae,” *European Journal of Mechanics-B/Fluids* **41**, 81–93 (2013).
- ¹⁸M. K. Panda and S. Ghorai, “Penetrative phototactic bioconvection in an isotropic scattering suspension,” *Physics of Fluids* **25**, 071902 (2013).
- ¹⁹M. K. Panda and R. Singh, “Penetrative phototactic bioconvection in a two-dimensional non-scattering suspension,” *Physics of Fluids* **28**, 054105 (2016).
- ²⁰M. K. Panda, R. Singh, A. C. Mishra, and S. K. Mohanty, “Effects of both diffuse and collimated incident radiation on phototactic bioconvection,” *Physics of Fluids* **28**, 124104 (2016).

- ²¹M. K. Panda, “Effects of anisotropic scattering on the onset of phototactic bioconvection with diffuse and collimated irradiation,” *Physics of Fluids* **32**, 091903 (2020).
- ²²M. K. Panda, P. Sharma, and S. Kumar, “Effects of oblique irradiation on the onset of phototactic bioconvection,” *Physics of Fluids* **34**, 024108 (2022).
- ²³M. K. Panda and S. K. Rajput, “Phototactic bioconvection with the combined effect of diffuse and oblique collimated flux on an algal suspension,” *Physics of Fluids* **35** (2023).
- ²⁴S. Rajput and M. Panda, “Effect of scattered/diffuse flux on the phototactic bioconvection in the absence of collimated flux,” *Physics of Fluids* **36** (2024).
- ²⁵J. R. Cash and D. R. Moore, “A high order method for the numerical solution of two-point boundary value problems,” *BIT Numerical Mathematics* **20**, 44–52 (1980).
- ²⁶H. Wager, “Vii. on the effect of gravity upon the movements and aggregation of euglena viridis, ehrb., and other micro-organisms,” *Philosophical Transactions of the Royal Society of London. Series B, Containing Papers of a Biological Character* **201**, 333–390 (1911).
- ²⁷S. Kitsunozaki, R. Komori, and T. Harumoto, “Bioconvection and front formation of paramecium tetraurelia,” *Physical Review E* **76**, 046301 (2007).
- ²⁸J. O. Kessler, “Co-operative and concentrative phenomena of swimming micro-organisms,” *Contemporary Physics* **26**, 147–166 (1985).
- ²⁹C. R. Williams and M. A. Bees, “A tale of three taxes: photo-gyro-gravitactic bioconvection,” *Journal of Experimental Biology* **214**, 2398–2408 (2011).
- ³⁰J. Kessler, “Path and pattern—the mutual dynamics of swimming cells and their environment,” *Comments Theor. Biol.* **1**, 85–108 (1989).
- ³¹D.-P. Häder, “Polarotaxis, gravitaxis and vertical phototaxis in the green flagellate, euglena gracilis,” *Archives of microbiology* **147**, 179–183 (1987).
- ³²B. Straughan, *Mathematical aspects of penetrative convection* (CRC Press, 1993).
- ³³S. Kumar, “Phototactic isotropic scattering bioconvection with oblique irradiation,” *Physics of Fluids* **34**, 114125 (2022).
- ³⁴N. A. Hill and D.-P. Häder, “A biased random walk model for the trajectories of swimming micro-organisms,” *Journal of theoretical biology* **186**, 503–526 (1997).
- ³⁵J. O. Kessler, “The external dynamics of swimming micro-organisms,” *Progress in phycological research* **4**, 258–307 (1986).
- ³⁶J. O. Kessler and N. A. Hill, “Complementarity of physics, biology and geometry in the dynamics of swimming micro-organisms,” in *Physics of biological systems* (Springer, 1997) pp.

- 325–340.
- ³⁷A. Kage, C. Hosoya, S. A. Baba, and Y. Mogami, “Drastic reorganization of the bioconvection pattern of chlamydomonas: quantitative analysis of the pattern transition response,” *Journal of Experimental Biology* **216**, 4557–4566 (2013).
- ³⁸N. H. Mendelson and J. Lega, “A complex pattern of traveling stripes is produced by swimming cells of bacillus subtilis,” *Journal of bacteriology* **180**, 3285–3294 (1998).
- ³⁹S. M. Gittleson and T. L. Jahn, “Pattern swimming by polytomella agilis,” *The American Naturalist* **102**, 413–425 (1968).
- ⁴⁰N. S. Khan, T. Gul, M. A. Khan, E. Bonyah, and S. Islam, “Mixed convection in gravity-driven thin film non-newtonian nanofluids flow with gyrotactic microorganisms,” *Results in physics* **7**, 4033–4049 (2017).
- ⁴¹T. Hayat, A. Alsaedi, *et al.*, “Development of bioconvection flow of nanomaterial with melting effects,” *Chaos, Solitons & Fractals* **148**, 111015 (2021).
- ⁴²F. P. Incropera, T. R. Wagner, and W. G. Houf, “A comparison of predictions and measurements of the radiation field in a shallow water layer,” *Water Resources Research* **17**, 142–148 (1981).
- ⁴³K. J. Daniel, N. M. Laurendeau, and F. P. Incropera, “Prediction of radiation absorption and scattering in turbid water bodies,” (1979).
- ⁴⁴N. A. Hill, T. J. Pedley, and J. O. Kessler, “Growth of bioconvection patterns in a suspension of gyrotactic micro-organisms in a layer of finite depth,” *Journal of Fluid Mechanics* **208**, 509–543 (1989).
- ⁴⁵M. F. Modest and S. Mazumder, *Radiative heat transfer* (Academic press, 2021).
- ⁴⁶S. Chandrasekhar, “Radiative transfer dover publications inc,” New York (1960).
- ⁴⁷S. Ghorai and R. Singh, “Linear stability analysis of gyrotactic plumes,” *Physics of Fluids* **21**, 081901 (2009).
- ⁴⁸W. H. Press, “Numerical recipes in fortran.” *The Art of Scientific Computing*. (1992).
- ⁴⁹S. Kumar, “Isotropic scattering with a rigid upper surface at the onset of phototactic bioconvection,” *Physics of Fluids* **35**, 024106 (2023).
- ⁵⁰S. Kumar, “Effect of rotation on the suspension of phototactic bioconvection,” *Physics of Fluids* **35** (2023).

